

Analysis of Loss of Offsite Power Transient Using RELAP5/MOD1/NSC;

I: KNU1 Plant Transient Simulation

Hho Jung Kim · Bub Dong Chung · Young Jin Lee and Jin Soo Kim

Korea Advanced Energy Research Institute

(Received March 12, 1986)

RELAP5/MOD1/NSC를 이용한 원자력 1호기 외부전원상실 사고해석

I. 실제 사고해석

김호정 · 정법동 · 이영진 · 김진수

한국에너지연구소

(1986. 3. 12 접수)

Abstract

System thermal-hydraulic parameters and simulated, using the best-estimate system code(RELAP5/MOD1/NSC), based upon the sequence of events for the KNU1 (Korea Nuclear Unit 1) loss of offsite power transient at 77.5% power which occurred on June 9, 1981. The results are compared with the actual plant transient data and show good agreements. After the flow coastdown following the trips of both reactor coolant pumps, the establishment of natural circulation by the temperature difference between the hot and the cold legs is confirmed. The calculated reactor coolant flowrate closely approximates the plant data indicating the validity of relevant thermal-hydraulic models in the RELAP5/MOD1/NSC. Results also show that the sufficient heat removal capability is secured by the appropriate supply of the auxiliary feedwater without the operation of S/G PORVs.

In addition, a scenario accident at full power, based upon the same sequence of events described above, is also analysed and the results confirmed that the safety of KNU1 is secured by the appropriate operation of the S/G PORVs coupled with the supply of auxiliary feedwater which ensures sufficient heat removal capability. The characteristics of the non-safety related components such as the turbine stop valve closing time, S/G PORV settings etc. are recognized to be important in the transient analyses on a bestestimate basis.

요 약

1981년 6월 9일 원자력 1호기에서 발생한 77.5% 출력상태에서의 외부전원상실사고를 열, 수력학 적최적계산용 코드인 RELAP5/MOD1/NSC를 사용하여 모의하였으며 해석결과를 발전소 실측자료와

잘 일치하였다. 원자로 냉각재펌프의 트립에 따른 flow coastdown 후에 hot-cold leg 온도차에 의하여 자연순환 유동이 형성됨이 확인되었으며 실측자료와 잘 일치하여 이와 관련된 전산코드의 열수력학적모델의 타당성을 입증할 수 있었다. 또한 위의 사고전개가 정상운전상태인 전출력(100%)에서 재발하였을 경우를 가정하여 해석하였다. 이러한 해석을 통하여 보조급수의 공급과 더불어 증기발생기 PORV의 적절한 작동으로 원자력 1호기 노심잔열을 제거하여 안전성에 문제점을 야기하지 않음을 입증하였다. 최적 계산방법에 의한 사고해석에서는 turbine stop valve 작동시간, 증기발생기 PORV 설정치 등 non-safety 관련요소들의 특성에대한 정확한 모의가 필수적이다.

1. Introduction

Recent concerns and interests are of the full understanding and the prediction of the system thermal-hydraulic performances during plant transient in the efforts to quantitatively evaluate the performances during the progression of the transients. Therefore, the use of the advanced T/H codes has been promoted by the increasing trend to perform the transient analysis on a best-estimate basis.

Formerly, the tendency was to insert conservatism wherever uncertainties existed and/or information was judged to be lacking or under argument. This approach to modeling, which has a number of inherent advantages including simplicity and a firm framework for safety assessments, was intended to ensure a conservative prediction of plant behaviour.

With the increasing emphasis on transient analysis, the accurate prediction of the plant response becomes more and more important, as described above. Use of the advanced best-estimate codes for safety analysis requires, however, that its uncertainties be identified by the various ways of assessment, and be eliminated through the relevant updated technology, if possible. In other words, the capability of the code to accurately predict the plant behaviour should be confirmed.

Addressing the above point has been realized in many international research plans and one of the prime examples of this is the 'International

T/H Code Assessment and Applications Programs' coordinated by USNRC (Odar & Bessette; 1985). The goal of the program is to provide well-assessed and accurate codes for use in the plant safety-related studies by international cooperation and resource sharings.

The present study follows up this trend and deals with the best-estimate calculation method in transient analysis, using the RELAP5/MOD1/NSC developed through some modifications of the interphase drag and the wall heat transfer modeling routines of the RELAP5/MOD1/CY 018. As a first step in this series of analyses, an analysis on the KNU1 (Korea Nuclear Unit 1) loss of normal feedwater transient has already been carried out (Kim, et al.; 1986). As a follow-up, system thermal-hydraulic parameters are simulated based upon the sequence of events for the KNU1 loss of offsite power transient which occurred on June 9, 1981 and compared with the plant transient data.

Main objectives of the analysis are, first, to assess the best-estimate system code, RELAP5/MOD1/NSC, and second, to evaluate the effects of the actuation and the functioning of the safety and/or non-safety related components.

2. Plant and Sequence Description

The KNU1 is a 587 MWe two-loop Pressurized Light Water Reactor which consists of Westinghouse nuclear steam supply system (NSSS) and GEC turbine-generator. The reactor coolant system (RCS) is composed of a reactor vessel,

two inverted U-tube steam generators (S/Gs), two water-sealed reactor coolant pumps (RCPs), a pressurizer (PZR) and various inter-connecting pipings. The two heat transport loops of the system are designated loop-A and loop-B, and the pressurizer is connected, via a surge-line, to loop-A.

Plant Transient Sequence

Plant transient sequence is based upon the sequence of events record (1981) obtained from the plant. At around 11 : 00 AM on June 9, 1981, while operating at 77.5% reactor power and 447 MWe generator power, the I/I converter (LM-461A) of the S/G-A level control system malfunctioned generating a spurious signal that indicated high S/G-A water level. This signal activated the closure of the S/G-A main feedwater control valve (IFV-466) which subsequently caused the steam/water flow mismatch signal to be generated. The resulting S/G low level signal brought about the reactor/turbine trip at 11 : 05.20 AM. The turbine-generator continued to operate for 30 seconds, as

designed, and then tripped at 11 : 05.50 AM. At the moment of generator trips, the automatic transfer to the offsite power supply (154KV) should have occurred. However, both the automatic and the manual transfer of Bus-A failed, whereas Bus-B succeeded in automatic transfer to the offsite power initially but also failed after 31 seconds. Both buses were open at 11 : 06.21 AM.

Failure of Bus-A caused the RCP-A to trip at 11 : 05.55 AM immediately followed by the actuation of the diesel generator-A (D/G-A) which provides emergency power to safeguard Bus-A. The failure of Bus-B after the initial successful transfer caused a loss of offsite power transient for about 6 minutes from 11 : 06.21 AM. The failure of Bus-B caused the RCP-B to trip at 11 : 06.23 AM and the D/G-B to begin supplying power to safeguard Bus-B. After 6 minutes into the loss of offsite power transient, at 11 : 11.52 AM, Bus-B recovered the offsite power and subsequently the D/G-B was manually tripped. Despite the recovery of offsite

Table 1. Sequence of Events for Plant Transient(1981. 6. 9)

Time(sec)	Initiating Events	Simulated Events
0. 0	—77. 5% Power Operation	—Steady State Calculation
50. 0	—Mal-function of I/I Converter S/G 'A' MFWCV starts to close	—Accident Sequence Starts —Use Plant Data in Main Feedwater Flowrate
100. 0	—S/G 'A' Low level & S/W mismatch Reactor/TBN Trip	—Reactor Trip(99. 438 sec) Turbine stop valve close
103. 81		—S/G 'A' L-level & Tavg<563. 0 K
105. 88		—S/G 'B' MFWCV starts to close
125. 88		—S/G L-L Level
130. 00	—Electric Generator Trip 2 Emergency D/G in Operation	—Auxiliary Feedwater Starts to Feed
131. 00	—154KV Bus-A Fail to Transfer —154KV Bus-B Succeed to Transfer	
135. 00	—RCP-A Trip	—RCP-A Trip (134. 44 sec)
137. 00	—Safeguard Bus-A in Operation	
161. 00	—154KV Bus-B Fail	
163. 00	—RCP-B Trip	—RCP-B Trip (162. 50 sec)
165. 00	—Safeguard Bus-B in Operation	

power in Bus-B, the RCP-B continued to remain tripped until it was manually activated at 11 : 32 AM. Recovery of offsite power to Bus-A was achieved much later and the RCP-A was re-activated at 07 : 16 PM.

In summary, from 11 : 06.23 to 11 : 32, both RCPs were not in operation causing a complete loss of reactor coolant flow accident for 26 minutes, and from 11 : 05.51 to 11 : 06.21 and also from 11 : 32 to 19 : 16, only one RCP was operating causing a partial loss of reactor coolant flow accident. Major sequence of events of the transient is summarized in Table 1 together with the simulated boundary conditions of the sequence.

Scenario Accident Sequence

The sequence of events for plant transient (at 77.5% power) described above was used as the basis for the scenario accident sequence. Generally, in this type of accidents (Decrease in Heat Removal by the Secondary System), the higher the power, the more serious is the accident. Hence, a scenario accident with identical sequence of events as the plant transient analysis was analyzed for 100% reactor power. This is because the reactor is normally operated at full reactor power and therefore this type of accident

Table. 2. Sequence of Events for Scenario Accident

Time (sec)	Simulated Events
0.00	—Steady State Calculation
50.00	—Accident Sequence Starts S/G-A MFWCV starts to close
96.13	—S/G-A low level & S/W mismatch Reactor/Turbine Trip Turbine Stop Valve close
101.75	—S/G-A low level & $T_{avg} < 563.0$ K S/G-B MFWCV starts to close
121.75	—S/G-A L-L Level —Aux. Feedwater starts to feed
131.13	—RCP-A Trip
138.00	—S/G PORV open and start to cycle
159.13	—RCP-B Trip

is most likely to occur at this power. The sequence of events used in this analysis is summarized in Table 2.

3. Code and Input Model Description

Code Description

The RELAP5/MOD1/NSC used in the analysis is best-estimate thermal-hydraulics computer code for system transient analyses of the Pressurized Water Reactors. The code was developed from the RELAP5/MOD1/CY018 (Ransom, et al.; 1981) by modifying some of the thermal-hydraulic models to avoid an unphysical flow oscillation. These modifications involve two-phase flow regime map, interphase drag and wall heat transfer models. Detailed description of the modified modeling routines can be found in Kim, et al. (1986).

Input Model

The KNU1 nodalization is shown in Fig. 1. The nodalization divides the whole system into 113 volumes including 11 boundary volumes, 117 junctions and 79 heat slabs. Each steam generator is modeled with 8 heat slabs for U-tubes and 13 volumes including a steam separator. The outlets of both S/Gs are connected to form a single volume, 'steam head', which is then connected to two time-dependent volumes that act as the pressure boundary conditions for the steam generators. More details can be found in Kim, et al. (1985).

Initial Conditions

RELAP5/MOD1/NSC steady-state calculations for 77.5% and 100% power were carried out to provide the initial conditions for the transient analyses. The simulated initial conditions along with the desired plant steady-state data for both power cases are summarized in Table 3 and Table 4. Generally the simulated values are in excellent agreement with the desired values. The simulated reactor power in both cases accurately

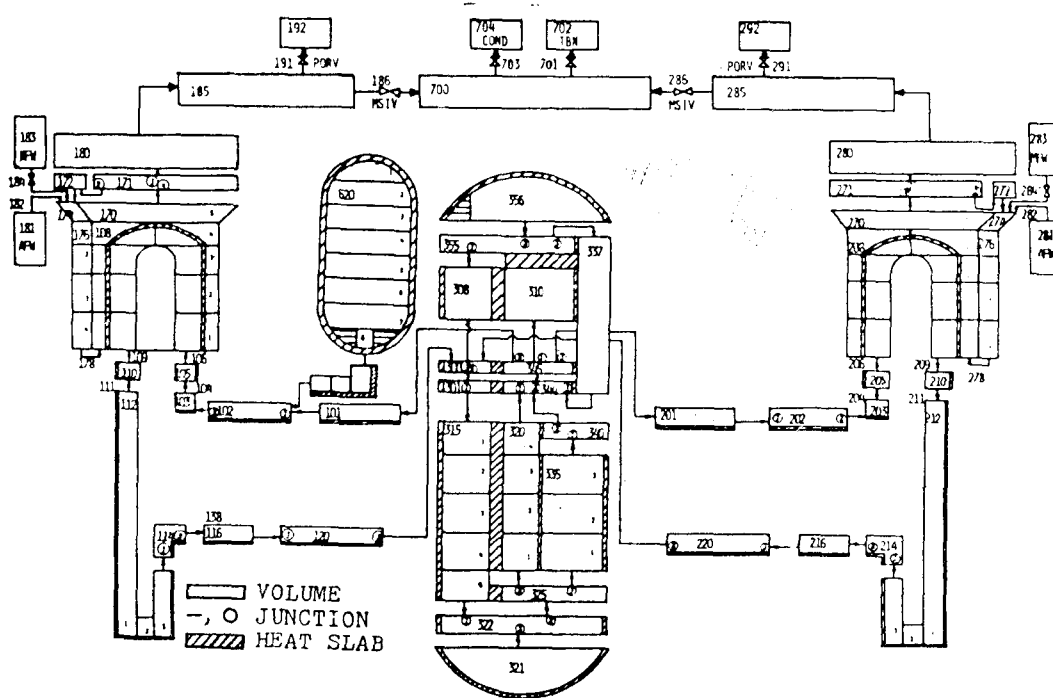


Fig. 1. RELAP5/MOD1/NSC Nodalization for KNU1 Accident Analysis

describes the desired power but the total heat transfer rate through the S/Gs, in both cases, is 2.9 MW higher than desired. This difference is caused by the reactor coolant pump model of the code which calculates more heat (2.9MW) than

desired. However this increase in the total heat transfer rate caused no significant deviations in other thermal-hydraulic parameters except for the expected slight increase (0.3kg/sec for 77.5 % and 0.8kg/sec for 100% power) in steam

Table. 3. Initial Conditions(77.5% Power)

Parameters	Simulated	Desired
Core Thermal Power(MW)	1,334.8	1,334.8
PZR Pressure(MPa)	15.50	15.41
PZR Level, Narrow Range(%)	41.17	41.60
Hot Leg Temperature(K)	583.20	583.10
Cold Leg Temperature(K)	556.90	556.80
Loop Coolant Flow(kg/sec)	4,687.4	4,686.5
Main Feedwater Flow(kg/sec)	356.70	356.70
Feedwater Temperature(K)	484.8	484.8
Steam Flow(kg/sec)	357.0	356.7
S/G Pressure(MPa)	5.838	5.804
S/G Narrow Range Level(%)	44.02	44.00
S/G Mass Inventory(kg)	46,294.6	—
U-tube Heat Transfer Area(m ²)	5,214.4	4,784.5
U-tube Heat Transfer Rate(MW)	1,342.7	1,339.8
Recirculation Ratio	4.52	—

Table. 4. Initial Conditions(100% Power)

Parameters	Simulated	Desired
Core thermal Power(MW)	1,723.5	1,723.5
PZR Pressure(MPa)	15.50	15.50
PZR Level(%)	46.73	47.60
Hot Leg Temperature(K)	589.41	589.36
Cold Leg Temperature(K)	555.94	555.89
Loop Coolant Flow(kg/sec)	4,687.5	4,687.5
Main Feedwater Flow(kg/sec)	473.10	473.10
Feedwater Temperature(K)	496.3	496.3
Steam Flow(kg/sec)	473.9	473.1
S/G Pressure(MPa)	5.55	5.55
S/G Narrow Range Level(%)	43.90	44.00
S/G Mass Inventory(kg)	44,313.1	44,776.7
U-tube Heat Transfer Area(m ²)	5,214.4	4,784.5
U-tube Heat Transfer Rate(MW)	1,731.4	1,728.5
Recirculation Ratio	2.5	2.5

flow rate. Following the reactor trip, the decay heat becomes an important parameter in the transient analysis, and is dependent on the initial core thermal power. Hence the relatively small increase in the total heat transfer rate is expected to give little effect on the system thermal-hydraulic parameters throughout the whole transient period. Small deviations in the pressurizer level was found to have no significant effect on the transient events and timings, in the present simulation.

4. Results and Discussion

Analyses were performed following the sequence described above. The initiating and the major simulated events during the progression of the transients are summarized in Table 1 and Table 2 for 77.5% and 100% power, respectively. As can be seen in the tables, the sequence of events is identical in both cases but the timing of major events differs somewhat as expected. The simulated thermal-hydraulic parameters for 77.5% power are compared with the plant transient data, which are deduced from the computer daily log sheet and trip review sheet. The scenario accident analysis results (100% power) are also compared with those of the plant

transient in order to identify and evaluate the effect of power on the safety for such type of accidents.

The plant transient occurred during power escalation, and hence most parameters were not in stabilized conditions which led to difficulties in deciding the appropriate initial values. Hence, the unreasonable plant data were ignored and the initial values were chosen either by an averaging process, or in some cases, from the design values specified in the FSAR (Final Safety Analysis Report). In the initial stages of the plant transient, the main feedwater flow rate was automatically controlled by the MFWCV (Main Feed Water Control Valve) following the malfunction of the S/G level indicator. Since the actual automatic operation of the MFWCV is difficult to identify, the feedwater flowrate shown in Fig. 2 is taken from the plant data to simulated the operation of the MFWCV and hence defines a boundary condition. In the scenario accident analysis, the main feedwater flowrate is assumed to be proportionally higher in magnitude than that for the plant transient.

As can be seen in Table 1, the MFWCV for S/G-B starts to close according to the trip logic, i.e., S/G low level and $T_{avg} < 563.0K$. The simulated actuation timing of the MFWCV is identical

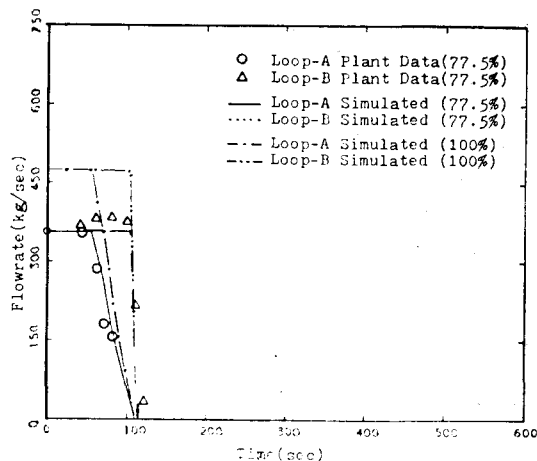


Fig. 2. S/G Feedwater Flowrate vs. Time

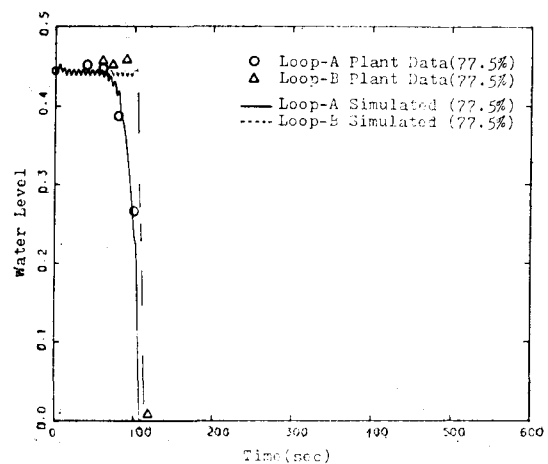


Fig. 3. S/G Water Level vs. Time

to the plant data leading to an accurate description of the feedwater flowrate. The increase in the S/G-B feedwater flow shown by the plant data during the initial stage of the transient may be caused by the unsteady feedwater flowrate due to the actions of the S/G level control system while increasing reactor power. The calculated S/G water levels agree well with the plant data as shown in Fig. 3. This indicates that the code responds well to the variation in the feedwater flowrate leading to the same reactor trip time. The increase in the S/G-B water in the level initial stage of the transient is thought to be due to the unstable feedwater flowrate discussed previously. The S/G water level was obtained not by the pressure difference method, as used in the actual plant measurement, but by calculating the collapsed water volume deduced from the void fraction. This is because the pressure difference method, when used in the simulation, often resulted in a doubtful level oscillation (Kim, et al.; 1986). Since the two loops of the S/G secondary side are connected via a single common head and because the main steam isolation valve (MSIV) does not operate in these analyses, the pressure variations in S/G-A and B are identical as shown in Fig. 4. Following the reactor/turbine trip, the S/G pressure rapidly increases as the turbine stop

valve closes. Normally, the turbine trip causes the steam dump valve to open. But in this transient, due to the loss of offsite power it remains closed. In the plant transient analysis, the S/G pressure starts to decrease as the supply of the auxiliary feedwater, which is actuated by the S/G low-low level signal, reaches its maximum capacity (155.88 sec) so that the secondary heat removal capability begins to overcome the reactor decay power. The calculated S/G pressure variation up to the peak pressure agrees quite well with the plant data but there exists noticeable differences in the subsequent pressure decrease following the actuation of the auxiliary feed. This difference may be expected because the analysis does not take into account the pressure drop due to the steam supply from the main steam line to the turbine driven auxiliary feedwater pump, nor the heat removal effect of the auxiliary feedwater fed by the turbine driven pump.

In the analyses, PORVs (Power Operated Relief Valves) were simulated to open at 7.033 MPa (1020 psia) in order to maintain the S/G pressure to a certain limit. But the supply of the auxiliary feedwater alone secures sufficient secondary heat removal capability without the operation of the PORVs. In the scenario accident sequence analysis, the pressure increase after the reactor/turbine trip does show similar trends, but in contrast to the plant transient case, the supply of the S/G auxiliary feedwater alone is not sufficient to remove the core decay heat. Insufficient heat removal causes the S/G pressure to increase up to the PORV set point and it remains there throughout the whole transient. The steam flow through the PORVs is found to cycle while exponentially decreasing in magnitude. The steam flow through the PORVs coupled with the auxiliary feedwater sufficiently improves the secondary heat removal capacity so that the core decay heat and the secondary heat removal become balanced.

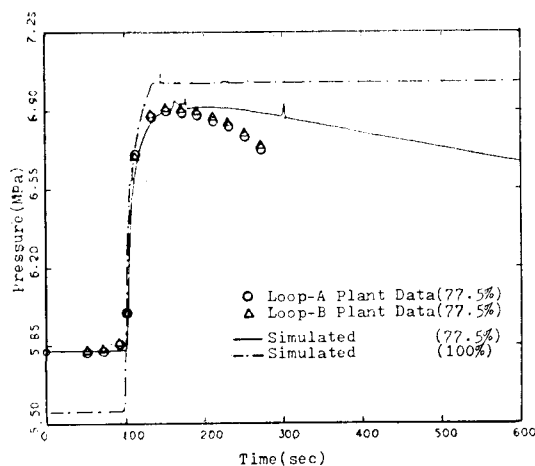


Fig. 4. S/G Steam Pressure vs. Time

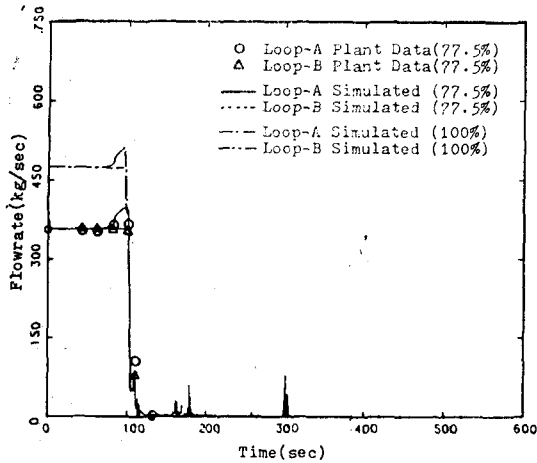


Fig. 5. S/G Steam Flowrate vs. Time

The calculated rapid reduction in the S/G steam flowrate following the reactor/turbine trip is in good agreement with the plant data (Fig. 5). The increase in S/G-A steam flowrate in the early stage of the transient is due to the liquid in the S/G downcomer changing its state from sub-cooled to saturated following the reduction in the main feedwater flowrate. In addition, the steam flowrate experiences a little unphysical oscillations which may be because the hysteresis effect in the interphase drag calculation is not considered and the separator model is not accurately describing the actual phenomena. This was also recognized in the loss of main feedwater transient analysis (Kim, et al.; 1986).

The primary loop coolant flowrate versus time is shown in Fig. 6, and as shown in Table 1 and Table 2, the reactor coolant pump-A (RCP-A) tripped at 135sec (131.13sec for scenario accident) and the RCP-B at 163sec (159.13sec for scenario accident). In both cases, the rapid reduction in the RCS flowrate in loop-A due to the pump trip caused the total RCS flowrate to increase, resulting in a decrease in the frictional resistance of the reactor vessel. Consequently the loop-B coolant flowrate increases until the subsequent trip of the RCP-B leading to the rapid reduction of loop-B flowrate. Meanwhile,

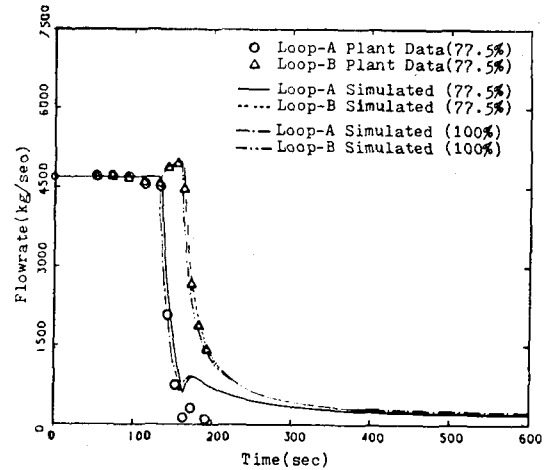


Fig. 6. Loop Coolant Flowrate vs. Time

the loop-A flowrate increases, due to the same reason as described above, just before flow reversal occurs and then decreases slowly. After 200 second, both loops show identical trend in the flow coastdown and the natural circulation begins to be established due to the hot-cold leg temperature difference. The overall trend in the calculated loop flowrates is in excellent agreement with the plant data as can be seen in Fig. 6. In addition, the RCS flowrates of the scenario accident show a similar trend to the plant transient analysis except a slight increase in magnitude of the stable natural circulation. This is expected since the decay heat is higher for 100% power resulting in larger hot-cold leg temperature difference.

Fig. 7 shows the RCS temperature variations and one can note that the hot leg temperature variations for both loops are identical in spite of different RCP trip times. This is reasonable since the present simulation deals with a single channel model for the core, allowing complete liquid mixing. Immediately following the reactor/turbine trips the hot leg temperature decreases rapidly, whereas the cold leg temperature increases due to the reduction in the heat removal capability which is caused by the increase in the secondary side S/G pressure as described above.

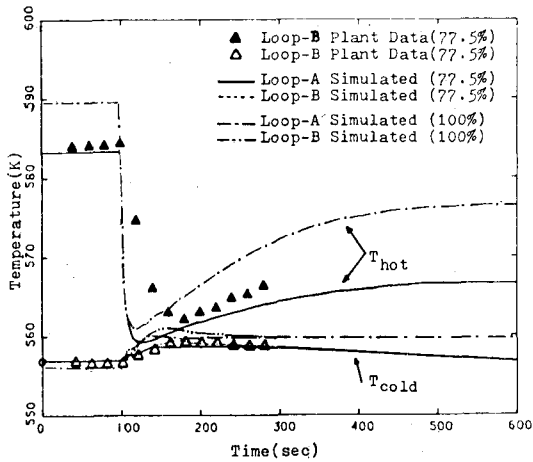


Fig. 7. Loop Coolant Temperature vs. Time

After the RCP-A trip, loop-A hot leg temperature has little effect on the cold leg temperature due to the delay in fluid transport and hence the cold leg temperature stays at the saturation temperature corresponding to the S/G-A pressure. Similarly, the loop-B cold leg temperature also ceases its increase following the RCP-B trip. Afterwards, the cold leg temperatures slowly decrease as the S/G pressure decreases. The flow coastdown due to both RCP trips as well as the decay heat increases the hot-cold leg temperature difference until the establishment of the natural circulation in the primary side due to this temperature difference gives rise to sufficient heat transfer capability from the primary to the secondary side(550sec). Recognizing above trend in the temperature variations, one can note that the hot leg temperature increases until the stable natural circulation is fully established, and afterwards it decreases as the cold leg temperature. The simulated cold leg temperature agrees well with the plant data whereas the hot leg temperature, although showing similar trend, is slightly lower in magnitude. This may be expected since the initial hot leg temperature used in the simulation is about 1.5K lower and the plant data involve measurement uncertainties. The results of the scenario accident analysis

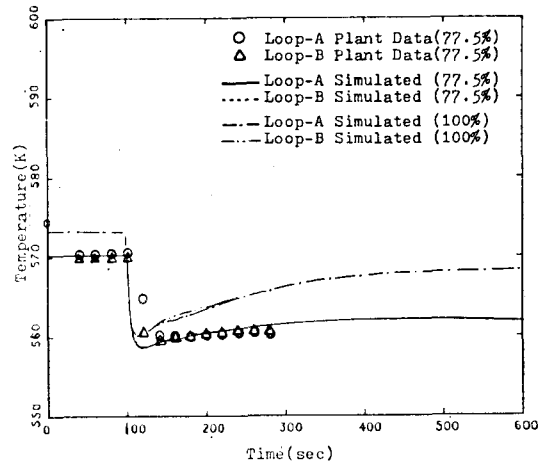


Fig. 8. Loop Coolant Average Temperature vs. Time

show similar trends in the hot and the cold leg temperatures to the plant transient analysis. However, as expected, the hot leg temperature stabilizes at a higher value because of the higher decay power corresponding to higher initial reactor power, as described above. The cold leg temperature, which is influenced by the S/G secondary side pressure, remains at the saturation temperature of the PORV setting pressure.

RCS average temperature shown in Fig. 8 agrees well with the plant data. However, the simulated temperature shows a slow increase after the rapid reduction following the reactor/

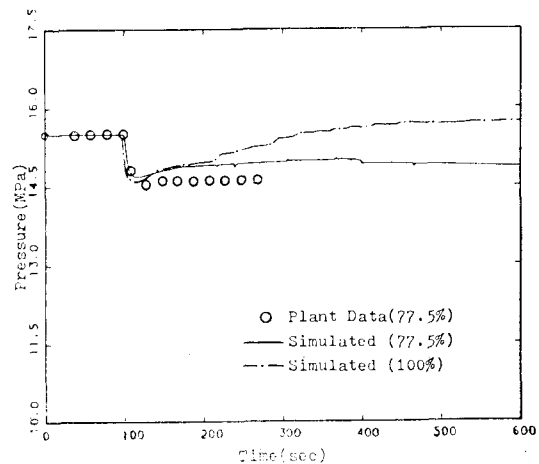


Fig. 9. Pressurizer Pressure vs. Time

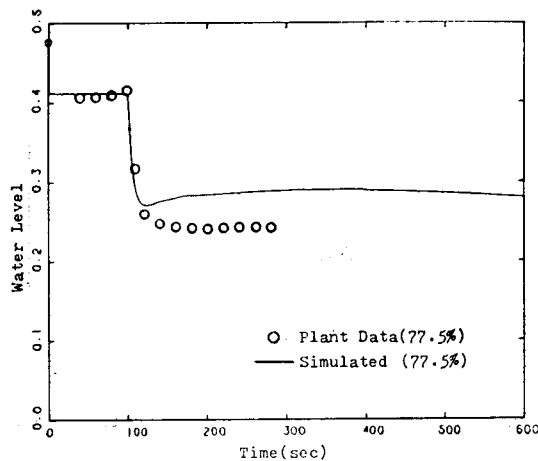


Fig. 10. Pressurizer Level vs. Time

turbine trip whereas the plant data remains almost constant. This is due to the under-estimation of the secondary heat removal capability, in the present simulation, as already discussed for Fig. 4. This phenomenon is also noted in pressurizer pressure and level as can be observed in Fig. 9. and Fig. 10 respectively. In the scenario accident analysis, the RCS average temperature stabilizes at higher temperature, as expected.

5. Conclusion

An analysis of KNU 1 loss of offsite power transient was carried out using the RELAP5/MOD1/NSC. It is found that the code gives stable steady-state results and accurate predictions of the plant behaviour for the transient, indicating the excellent capability of the code for this type of transients. The establishment of stable natural circulation due to the hot-cold leg temperature difference after both reactor trips is confirmed. In particular, the calculated RCS flowrate closely follows the plant data and this validates that the relevant thermal-hydraulic models in RELAP5/MOD1/NSC are correctly describing the actual phenomena.

Results also show that the sufficient heat removal capability is secured by the appropriate supply of the auxiliary feedwater without the operation of S/G PORVs. In addition, the results for a scenario accident at full power confirm that the appropriate operation of the S/G PORVs coupled with the supply of auxiliary feedwater ensures sufficient heat removal capability and therefore no hazard to the reactor is imposed.

The characteristics of the non-safety related components such as the turbine stop valve closing time, S/G PORV settings etc. are recognized to be important in the transient analyses on the best-estimate basis.

References

1. Computed Daily Log Sheet of KNU1, on June 9, 1981.
2. Computed Post Trip Review Sheet of KNU1, 11:00 on June 9, 1981.
3. Computer Sequence of Events Record of KNU1, 11:00 on June 9, 1981.
4. "Final Safety Analysis Report, Ko-Ri Nuclear Power Plant Unit No.1", Korea Electric Company.
5. Kim, H.J., et al., "KNU1 Input Deck Preparation Using RELAP5/MOD1/NSC", KAERI/NSC-147/85, 1985.
6. Kim, H.J., et al., "Analysis of Loss of Normal Feedwater Transient Using RELAP5/MOD1/NSC; KNU1 Plant Simulation", Journal of Korea Nuclear Society, Vol. 18, No. 1, 1986, pp.9~16.
7. Odar, F. & Bessette, D.E., "Guidelines and Procedures for the International Thermal-Hydraulic Code Assessment and Applications Program", presented at the 1st Meeting of the International T/H Code Assessment and Applications Program, Silver Spring, Maryland, 1985.
8. Ransom, V.H., et al., "RELAP5/MOD1 Code Manual", NUREG/CR-1826, EGG-2070 Draft Rev. 2, 1981.